ENGINEERING TRANSACTIONS • *Engng. Trans.* • **41**, 1, 77–96, 1993
Polish Academy of Sciences • Institute of Fundamental Technological Research

DISCRETE MODEL OF WAVE PROPAGATION IN A NONPRISMATIC BAR WITH RIGID UNLOADING CHARACTERISTICS

Z. SZCZEŚNIAK (WARSZAWA)

A discrete model is proposed for the propagation of waves in a nonprismatic bar made from a material whose unloading characteristic is rigid. Arbitrary time-dependent applied load is considered. In such a situation the modelling of wave propagation must allow in each cross-section for multiple effects of its alternating rigid and activated behaviour. These effects are nonlinear and thus it is very difficult to approach them analytically. An algorithm for numerical solutions is proposed and errors of the results are discussed. Effectiveness and applicability of the model are illustrated by means of numerical examples.

1. INTRODUCTION

The propagation of plastic waves must be formulated on the basis of a physical law which is different for loading and unloading processes. Experimental evidence shows that the unloading branches of the $\sigma - \varepsilon$ relationships for soils and some other media can be approximated by a rigid behaviour in a satisfactory manner [1÷3].

In the theoretical analyses the physical models of materials with rigid unloading have proved to be of considerable practical importance [4÷10, 18, 19, 21]. The use of such an unloading behaviour remarkably simplifies the solutions of a number of problems encountered in the engineering practice. Good agreement of some theoretical solutions with suitable test results was emphasized in [4, 6–8, 11]. The solutions refer to some particularly simplified patterns of applied load [4, 6, 7, 10, 11]. Arrival at solutions for arbitrarily variable applied load is fraught with serious difficulties. They result from the fact that the unloading process is described by a nonlinear differential equation with nonstationary boundary conditions, e.g. [18, 19].

This paper is devoted to the propagation of one-dimensional waves in materials with rigid unloading characteristics acted upon by time-dependent

edge loads. A bar with variable cross-section will be considered. A method will be presented that makes it possible to solve such a problem in an effective manner with the help of discretization procedures. Foundations of this discrete method for a linearly elastic material under both loading and unloading were presented in [12] and developed in [13].

An essential feature of the method is a discrete model whose structure and operation are based on the principle of errorless difference approximation. It is in this paper that an analogous discrete model is proposed capable of taking into account an additional effect of rigid unloading. The errorless difference approximation is preserved in the loading processes. Unfortunately, this principle cannot be applied in the processes of rigid unloading which ceases to have a wave characteristic. However, an effective way to minimize errors will be indicated.

The discrete model of this paper, along with the model described in [12], is of fundamental importance to construct complex discrete models for the wave propagations in the case of nonlinear $\sigma - \varepsilon$ relationships. A piece-wise linear approximation is used to reach effective solutions.

The described simple model can be applicable in the dynamic analysis of displacements of structures that interact with soils. The solutions of examples in Sec. 5 will be instructive in this respect.

2. Assumptions and general characteristic of the problem

Consider a semi-infinite nonprismatic bar whose material deforms according to the $\sigma - \varepsilon$ relationship shown in Fig. 1. Upon loading the material behaves as a linearly elastic one, whereas upon unloading its internal constraints make it impossible to deform, hence the rigid unloading behaviour.

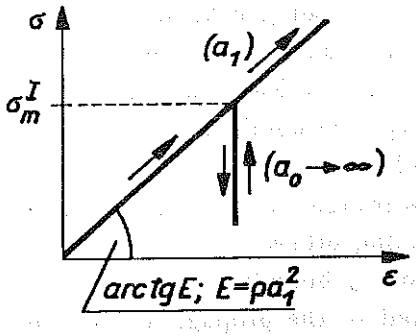

Fig. 1.

It is soils that behave in such a manner. Various models of soils have been described in the literature and broadly discussed in [3,4,14–21]. Soil is sometimes considered as a three-phase medium, not infrequently sensitive to strain rates. However, the constitutive law adopted in this paper does not allow for viscous effects.

A free end of the bar is acted upon by arbitrary, piece-wise monotonic load $p(t)$ (Fig. 2a). As a result, two neighbouring regions are created: a loading region I and a rigid unloading region II (Fig. 2d). The time-depen-

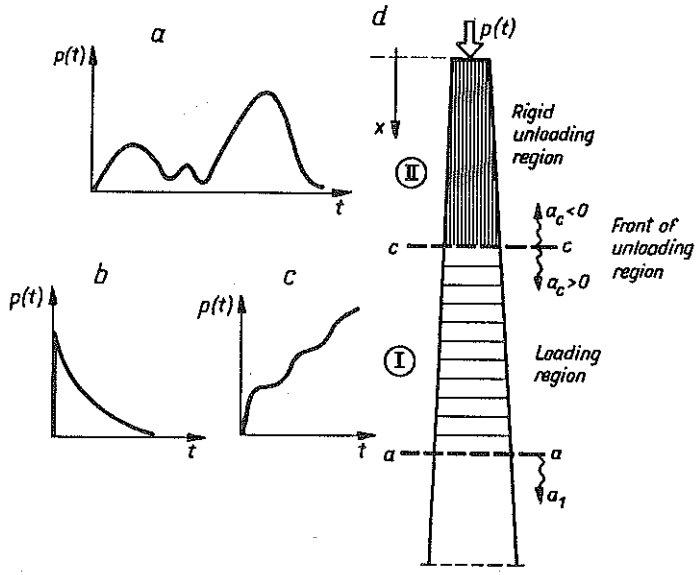

FIG. 2.

dent interfaces are denoted by $a-a$ and $c-c$. In the region I the considered problem is of wavy nature and is described by an equation, suitable for a bar with variable cross-section, namely

$$\frac{\partial^2 u}{\partial t^2} - a_1^2\left(\frac{\partial^2 u}{\partial x^2} + \frac{2}{x}\frac{\partial u}{\partial x}\right) = 0, \tag{2.1}$$

where $u = u(x,t)$ denotes a displacement, a_1 is the wave velocity in the loading process and is equal to $a_1 = (E/\varrho)^{1/2}$.

The cross-sectional area $A(x)$ of the bar varies according to the rule

$$\begin{aligned} A(x+dx) &= A(x) + dA(x), \\ dA(x) &= 2A(x)\frac{1}{x}dx. \end{aligned} \tag{2.2}$$

Suitable boundary conditions must be taken into account. A decreasing load $p(t)$ gives rise to an unloading process and a creation of region II. The strains cannot decrease due to the constraints assumed to be present in the material. This leads to a decay of wave propagation in the region II which becomes rigid and is subject to a rigid translation with the uniform velocity v_{II}. The motion equation for each element of the discussed region has the form

$$\varrho \frac{\partial v_{II}}{\partial t} = \frac{\partial \sigma}{\partial x} + \sigma(x)\frac{2}{x}. \tag{2.3}$$

The interface $c - c$ moves with a variable velocity a_c compatible with the dynamic states of the neighbouring regions. The signs of a_c characterize two different physical situations. Thus the two following cases take place

CASE 1. $a_c \geq 0$

During decreasing loading $p(t)$ the velocity v_{II} diminishes and the rigid region grows. The rigid region penetrates into the loading region and the latter shrinks. The course of the discussed process depends on the current dynamic parameters of the loading region.

CASE 2. $a_c \leq 0$

Increasing loading $p(t)$ causes an increase in the velocity v_{II} and the rigid region diminishes. A growth of the loading region takes place in accordance with the velocities a_1 and a_c. This effect will in what follows be called an activation of the rigid region. It is worth noting that the activation of a certain part of this region depends, among other reasons, on its state which was reached in the process of previous loading. Basic parameters of this state are: maximum stress $\overset{I}{\sigma}_m$, Fig. 1 and an associated mass velocity $\overset{I}{v}_m$.

An arbitrary loading as shown in Fig. 2a can cause that the same region of the bar will undergo multiple and alternating processes of activation and stiffening. In the particular case of loading shown in Fig. 2b rigidly unloaded region will propagate along the bar and a_c will equal a_1. In the case shown in Fig. 2c only the loading region will be present in the whole bar. From the above described situation it follows that in Eq. (2.3) we have two unknowns: velocity v_{II} and length of the region II. For their determination the continuity conditions at the interface $c - c$ are used

$$\overset{II}{v}_c = \overset{I}{v}_c, \qquad \overset{II}{\sigma}_c = \overset{I}{\sigma}_c. \tag{2.4}$$

In the case of stiffening the parameters $\overset{I}{v}_c$ and $\overset{I}{\sigma}_c$ are relevant for the loading

region. In the activation case it should be assumed that $v_c^{\mathrm{I}} = v_m^{\mathrm{I}}$ and $\sigma_c^{\mathrm{I}} = \sigma_m^{\mathrm{I}}$.

Allowance for an appropriate continuity condition leads to a differential equation in a nonlinear form. Closed-form solutions can only be obtained for simple loads $p(t)$.

3. Discrete model of a nonprismatic bar with rigid unloading characteristic

A discrete model of the interior of the considered bar is analogous to that described in [12]. It consists of a series of concentrated masses Δm_i as seen in Fig. 3. Motion of the masses is controlled by means of weightless constraints that are sensitive to the sign of displacement increment (velocity).

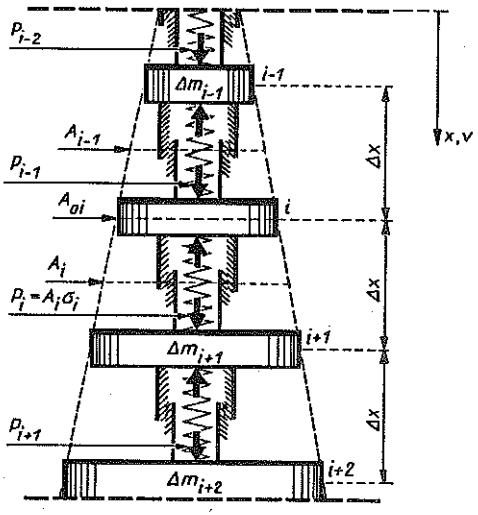

FIG. 3. $\Delta v_{i,i+1} = v_i - v_{i+1}$, 1. $\Delta v_{i,i+1} \geq 0$ – loading, 2. $\Delta v_{i,i+1} < 0$ cannot occur – rigid unloading.

These constraints can be visualized as "pike's teeth". Upon loading the springs are capable of deforming freely, whereas upon unloading the motion of springs is prevented by the system of locking teeth and no deformation occurs.

Operation of the described model at the loading stage is based on the criterion of errorless difference approximation [12]. This means that the spatial discretization Δx of the bar and the time discretization Δt satisfy

the formula $\Delta x = a_1 \Delta t$. The values of rigid masses in the discrete model should be determined according to the formula

$$\Delta m_i = A_{0i}\, a_1\, \Delta t \varrho, \tag{3.1}$$

where A_{0i} is a cross-sectional area of the bar at which the i-th mass is concentrated. This mass is acted upon by the forces P_i and P_{i-1} concentrated at constraints and resulting from the stresses σ_i and σ_{i-1} associated with the area A_i and A_{i-1}, respectively, see Fig. 3. In conformity with Eq. (2.2), these areas are calculated with the use of the following difference formulae

$$\begin{aligned} A_i &= A_{0i} + \Delta A, \\ A_{i-1} &= A_{0i} - \Delta A, \\ \Delta A &= 2A_{0i}\frac{1}{x_i}\frac{\Delta x}{2}. \end{aligned} \tag{3.2}$$

The performance of the considered model in the loading range is described by the following relationships:

$$\begin{aligned} \ddot{u}_i^{n,n+1} &= \frac{A_{i-1}\sigma_{i-1}^n - A_i\sigma_i^n}{m_i}, \\ \Delta u_i^{n,n+1} &= \Delta u_i^{n-1,n} + \ddot{u}_i^{n,n+1}\Delta t^2, \\ u_i^{n+1} &= u_i^n + \Delta u_i^{n,n+1}, \\ \sigma_{i-1}^{n+1} &= \frac{u_{i-1}^{n+1} - u_i^{n+1}}{\Delta x}E, \end{aligned} \tag{3.3}$$

where $\Delta u_i^{n,n+1}$ denotes a displacement increment of the i-th mass according to the parabolic approximation with respect to time.

The performance of the model in the rigid unloading range will be different due to the fact that an unloaded portion of the bar becomes undeformable. Moreover, the length of this portion can increase or decrease in accordance with the dynamic conditions of the considered problem. In these conditions operation of the model will be controlled by a suitable procedure for determining the length of rigid portion and its stresses.

A discrete model in the situation of growing rigid region is illustrated in Fig. 4. Dynamic parameters of the wave-front of the unloaded region at the level of the mass Δm numbered j will be denoted by the indices c, j. These parameters are: the velocity of wave-front of a rigid part $a_{c,j}^n$, mass velocity $v_{c,j}^n$ (constant over the whole rigid region) and the stress $\sigma_{c,j}^n$. The above parameters constitute the basic unknows of the problem under consideration.

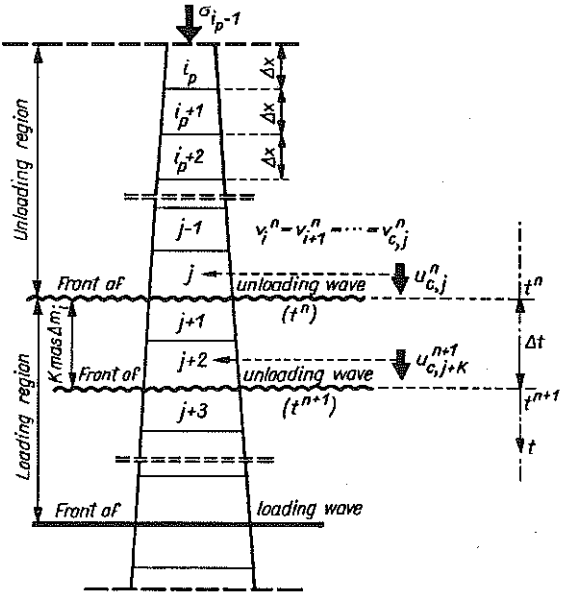

FIG. 4.

The velocity of the front of the unloaded region is, as a rule, variable and depends on the current dynamic parameters of the process. Variations in this velocity and, at the same time, in the length of the rigid region is characterized by a parameter $K = 1, 2, 3 \ldots$ that defines the distance $K\Delta x$ covered by the front of the considered region during the time step Δt. The parameter K will vary irregularly from one time step Δt to another because the mass velocities $v_{c,j}^n$ will vary too. The velocity $v_{c,j}^{n+1}$ at an instant t^{n+1} can be calculated from the momentum conservation principle. A uniform expression of this principle for the cases of stiffening and activation can be shown as follows:

$$v_{c,j+K}^{n+1}\,[M + \Delta M(K)] = M v_{c,j}^n + \Delta\pi^n(K) + \Delta P_x^n(K)\Delta t, \tag{3.4}$$

where

$$M = \sum_{i=i_p}^{i=j} \Delta m_i.$$

Specific forms of the remaining terms of the principle (3.4) for the two possible cases are the following:

CASE 1. Stiffening $\left(a^n_{c,j} \geq 0\right)$, the mass velocity $v^n_{c,j}$ diminishes:

$$
\begin{aligned}
\Delta M(K) &= \sum_{i=j+1}^{i=j+K} \Delta m_i, \\
\Delta \pi^n(K) &= \sum_{i=j+1}^{i=j+K} \Delta m_i v^n_i, \\
\Delta P^n_x(K) &= \sigma^n_{i_p-1} A_{i_p-1} - \sigma^n_{j+K} A_{j+K}.
\end{aligned} \tag{3.5}
$$

The stress σ^n_{j+K} and the velocities v^n_i are associated with the current region of loading.

CASE 2. Activation $\left(a^n_{c,j} \leq 0\right)$, the mass velocity $v^n_{c,j}$ grows:

$$
\begin{aligned}
\Delta M(K) &= -\sum_{i=j}^{i=j-K+1} \Delta m_i, \\
\Delta \pi^n(K) &= -\sum_{i=j}^{i=j-K+1} \Delta m_i v^n_{c,j}, \\
\Delta P^n_x(K) &= \sigma^n_{i_p-1} A_{i_p-1} - \sigma^n_{m,j-K} A_{j-K}.
\end{aligned} \tag{3.6}
$$

The stress $\sigma^n_{m,j-K}$ is at its maximum during the loading of the cross-section $j-K$.

It should be noticed that if $\Delta x \to 0$ and $\Delta t \to 0$, then $\Delta M(K) \to 0$, $\Delta \pi^n(K) \to 0$, $\Delta P^n_x(K) \to \dfrac{\partial \sigma}{\partial x} + \sigma \dfrac{2}{x}$, and the relationship (3.4) will be transformed to become a suitable differential expression (see Eq. (2.3)). This means that both the difference and the differential approaches to the considered problem coincide in the limiting case. The value of K in the formulae (3.4)–(3.6) is determined in an iterative manner. Starting from $K = 1$, consecutive positions of the front of the rigid region will be analysed so long as the calculated stress $\sigma^{n+1}_{c,j+K}$ or $\sigma^{n+1}_{c,j-K}$ will satisfy the following condition for the first time:

for stiffening

$$\sigma^{n+1}_{c,j+K} \geq \sigma^{\mathrm{I},n+1}_{j+K}, \tag{3.7}$$

for activation

$$\sigma^{n+1}_{c,j-K} \geq \sigma^{\mathrm{II},n+1}_{m,j-K}. \tag{3.8}$$

The stresses $\sigma_{c,j+K}^{n+1}$ for the stiffening are calculated with the help of the following set of relations

$$
\begin{aligned}
\ddot{u}_{c,j+K}^{n,n+1} &= \frac{v_{c,j+K}^{n+1} - v_{j+K}^{n}}{\Delta t}, \\
\Delta u_{c,j+K}^{n,n+1} &= \Delta u_{c,j+K}^{n-1,n} + \ddot{u}_{c,j+K}^{n,n+1} \Delta t^2, \\
u_{c,j+K}^{n+1} &= u_{c,j+K}^{n} + \Delta u_{c,j+K}^{n,n+1}, \\
\sigma_{c,j+K}^{n+1} &= \frac{u_{c,j+K}^{n+1} - u_{j+K+1}^{n+1}}{\Delta x} E,
\end{aligned}
\tag{3.9}
$$

where $\ddot{u}_{c,j+K}^{n,n+1}$, $\Delta u_{c,j+K}^{n+1}$, $u_{c,j+K}^{n+1}$ are the acceleration, the displacement increment and the displacement of the analysed mass $j+K$, respectively. For activation the indices $j+K$ should be replaced by $j-K$, and in Eq. $(3.9)_1$ the equality $v_{j+K}^{n} = v_{c,j-K}^{n}$ should be introduced. On calculating u_{j-K+1}^{n+1} in Eq. $(3.9)_4$ it should be remembered that the activation process takes place and thus the maximum stresses σ_m^{I} should be used, determined in the loading process.

For example, in the situation depicted in Fig. 4 the stresses in the rigid region $\sigma_{i_p}^{n+1} \div \sigma_{j+K-1}^{n+1}$ can be calculated from the expression

$$
\sigma_l^{n+1} A_l = \sigma_{l-1}^{n+1} A_{l-1} - \Delta m_l \frac{v_{c,j+K}^{n+1} - v_l^n}{\Delta t}, \tag{3.10}
$$

where $i_p \leq l \leq j+K-1$.

The boundary and the initial conditions should be formulated according to [12]. A general form of the boundary condition is obtained for a layered bar in this cross-section that separates the neighbouring segments with different impedances $a_r \varrho_r$ and $a_{r+1}\varrho_{r+1}$. In [12] the discussed condition was shown to be satisfied automatically provided in the discrete model the boundary mass Δm_{bi} will be

$$
\Delta m_{bi} = 0.5\,(\Delta m_{i,r} + \Delta m_{i,r+1}), \tag{3.11}
$$

where the index i numbers the cross-section in which the considered boundary mass is concentrated. The values of the constituent masses $\Delta m_{i,r}$, $\Delta m_{i,r+1}$ are calculated according to the formula (3.1).

From the condition (3.11) it follows that a free end of the bar in the discrete modelling should be associated with the mass of the value $\Delta m_{bi} = 0.5\Delta m_{i,r}$ since $a_{r+1}\varrho_{r+1} = 0$. The remaining masses will have the values $\Delta m_{i,r}$. In this situation the considered boundary mass cannot be directly

acted upon by an assumed discrete form $P_\Delta(t^n)$ of the applied load $p(t)$. This fact requires a special form of the load $P_z(t^n)$ to be determined. This is

$$(3.12)\quad P_z(t^n) = \begin{cases} 0.5P_\Delta(t^0), & \text{for } n = 0, \\ P_\Delta(t^{n-1}) - 0.5[P_\Delta(t^{n-1}) - P_\Delta(t^n)], & \text{for } n = 1,2,3,\ldots. \end{cases}$$

When the load is transmitted without paying attention to the effects of wave reflection (from the free end within the bar), the boundary mass can be equal to $\Delta m_{i,r}$ and it can be acted upon directly by the load in the form $P_\Delta(t^n)$.

Assuming $A(x) = \text{const}$, the considered model will be suitable for any prismatic bar.

4. Accuracy of the proposed model

The described discrete model operates in the loading process in the same manner as a linearly elastic model dealt with in [12]. In that paper it was indicated that the condition $\Delta x = a_1 \Delta t$ ensured an analysis of the loading process to within the accuracy of truncation errors. Such an accuracy cannot, however, be achieved for the unloading process. In general, the spatial and temporal course of the unloading process is nonlinear and that is why a determined location of the front of the unloading wave $l_{c,j+K} = (j + K)\Delta x$ does not necessarily have to coincide with the exact solution. This remark also applies to all parameters relevant to the front of the unloading wave. In the discussed situation the truncation errors are impossible to be avoided, although an effort can be made to make them as small as possible. Numerical analysis of the considered problem shows that a finer space-time discretization is a very effective way to minimize the errors. The computational algorithm presented in Sec. 3 also appears to be very effective. Solution to a given problem is therefore easy to obtain for various space-time discretizations and its convergence can be analysed with relative ease.

An exact solution to the considered problem as applied to a nonprismatic bar does not exist in the available literature. Thus the values of errors and possibilities of their minimization will be discussed for a bar with constant cross-section. An exact solution for this specific case is presented in [6]. A semi-infinite bar made of a material with rigid unloading characteristics is considered. At the end $x = 0$ the load $p(t)$ initially increases linearly in time and, at the instant τ, decays in an abrupt manner, Fig. 5. Two unknowns

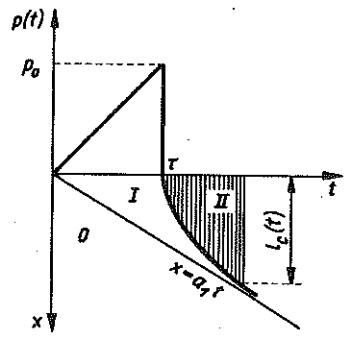

FIG. 5.

are sought: variable length of the rigidly unloaded part and the stress at its front. The following numerical data are assumed:

$$p_0 = 0.095\,\text{MPa}, \quad \tau = 0.125\,\text{s}, \quad a_1 = 101.4\,\text{m/s}, \quad \varrho_1 = 1800\,\text{kg/m}^3.$$

The exact solution [6] shows that under the assumed load $p(t)$ the front of the rigidly unloaded part propagates with fast varying velocity, especially at the initial stage starting from the time $t = \tau$. This situation appears to be particularly unfavourable for the attainment of high precision of the numerical solution.

The problem is solved by a suitable construction of a discrete model according to the rules presented in Sec. 3. All the concentrated masses have the same values, namely $\Delta m = a_1 \varrho_1 \Delta t$.

The solution for $0 \leq t \leq \tau$ (loading process) will bear the truncation errors only.

For $t > \tau$ the errors of the solution were analysed associated with the length of the unloaded part l_c of the bar and the stress σ_c at the front. The errors are defined as follows:

1) error $\delta^n(l_c)$ of the length l_c

$$\delta^n(l_c) = \frac{l^n_{c,D} - l^n_{c,N}}{l^n_{c,D}} \cdot 100,$$

2) error $\delta^n(\sigma_c)$ of the stress σ_c

$$\delta^n(\sigma_c) = \frac{\sigma^n_{c,D} - \sigma^n_{c,N}}{\sigma^n_{c,D}} \cdot 100,$$

where $l^n_{c,D}$, $\sigma^n_{c,D}$ – the values obtained from the exact solution for $t = n\Delta t$; $l^n_{c,N}$, $\sigma^n_{c,N}$ – corresponding values taken from the numerical solution.

The obtained computational results for $\Delta x = 1.305\,\mathrm{m}$ are shown diagrammatically in Fig. 6 from which it is seen that the largest errors are present at the beginning of the unloading process and refer to the length of the unloaded region. These errors oscillate around zero and diminish in a rapid way. For the large step $\Delta x = 1.305\,\mathrm{m}$ the greatest error amounted to 9.1% and after 26 steps it did not exceed 1%. For $t = 150\ \Delta t$ its value was as small as -0.17%. Errors in stresses are seen not to exceed 0.5%. The above errors can still be made smaller by decreasing the spatial step Δx or an associated time step Δt. For instance, for $\Delta x_1 = 0.1\Delta x$ an initial error in length $\sigma^{n=1}(l_c)$ was reduced to -1.25%.

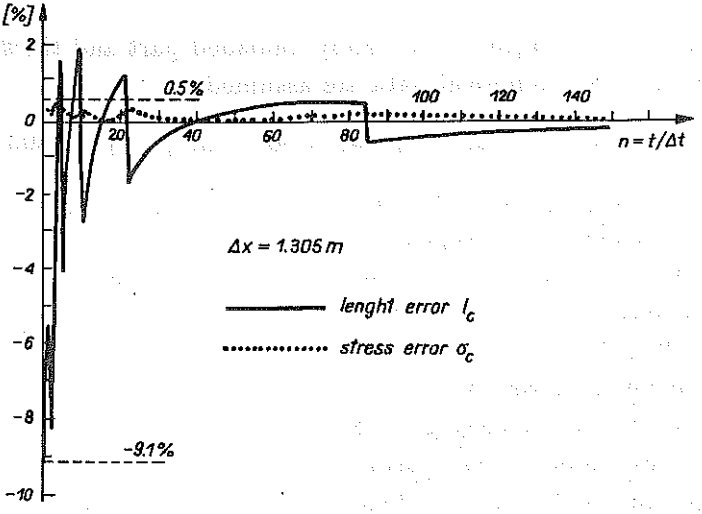

FIG. 6.

It should be also remembered that, due to the decay of the wave propagation process in the unloading region, the discussed errors are of a local character only.

In general, a proper choice of the steps Δx and Δt, resulting in an associated level of errors, depends upon individual conditions and requirements of a given problem.

In the engineering practice it often happens that the load $p(t)$ increases very abruptly to drop down according to an arbitrary function as is shown in Fig. 2b. Assume the load $p(t) = p_0(1 - t/\tau_1)$ to be applied at the free end of a semi-infinite prismatic bar, where $\tau_1 = 0.5\,\mathrm{s}$. The adopted data are: $a_1 = 104.4\,\mathrm{m/s}$ and $\varrho_1 = 1800\,\mathrm{kg/m^3}$. In the considered situation it is only the rigid region that exists in the bar since the loading region shrinks

to become a cross-section creating a front of the rigid region. The velocity of propagation of this front becomes equal to the velocity a_1. The length of the rigid region is determined in an exact manner. Certain errors are only involved in the calculations of the stresses σ_c^n. However, their values can hardly be noticed, see Table 1.

Table 1.

$i = \frac{x}{\Delta x}$	$\sigma_c^n(x)/p_0$; $\Delta x = 1.305\,\mathrm{m}$	
	exact solution	numerical solution
1	0.987500	0.987500
2	0.975001	0.975001
3	0.962501	0.962501
⋮	⋮	⋮
38	0.525014	0.525014
39	0.512514	0.512515
40	0.500014	0.500015

5. Numerical examples

Two examples will now be demonstrated. In the first one the effectiveness of the proposed method is studied for arbitrarily complex time-dependence of the applied load. In the other, an effect of variability of the cross-section of the bar on the displacements of undeformable mass through which the dynamic load is transmitted will be emphasized. The obtained results can be useful to select an appropriate computational model for the solution, for example, of dynamic motions of a structure interacting with soil.

Example 1

Consider a semi-infinite nonprismatic bar made from a material whose stress-strain relationship was depicted in Fig. 1. Variation of cross-sections is defined by the formulae (2.2). In conformity with Lubimov's method quoted in [22], variation of the cross-sectional area $A(x)$ is determined from the formula $A(x) = A_0 x/x_0^2$, where x_0 denotes an experimental parameter and $A_0 = A(0)$. Assume $A_0 = 1\,\mathrm{m}^2$. Material data are: $a_1 = 150\,\mathrm{m/s}$

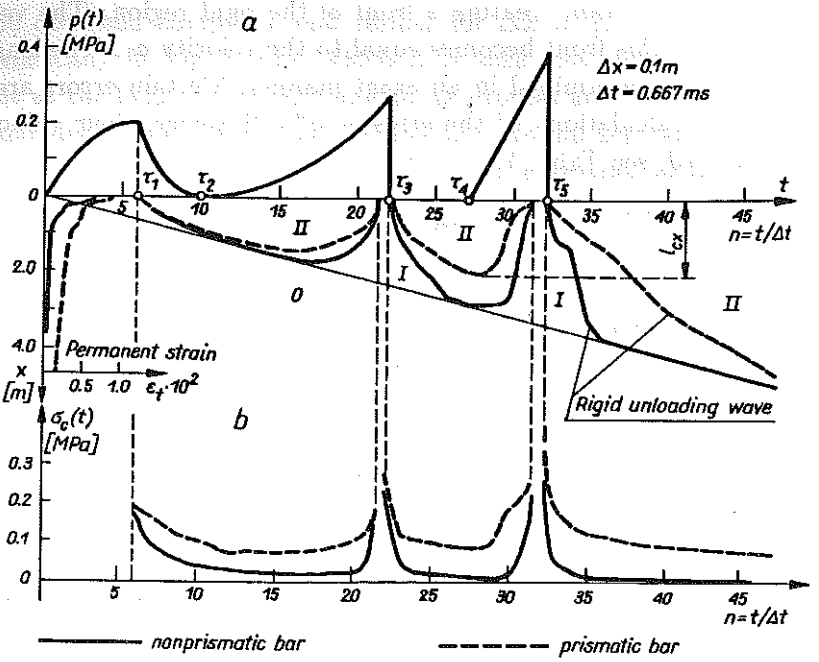

FIG. 7.

and $\varrho_1 = 1800\,\mathrm{kg/m^3}$. The free end of the bar is subjected to the following time-dependent load $p(t)$ (Fig. 7a):

$$(5.1)\qquad p(t) = \begin{cases} p_1(2\xi - \xi^2), \quad \xi = \dfrac{t}{\tau_1}, & \text{for } 0 \le t \le \tau_1, \\ p_1\left(\dfrac{\tau_2 - t}{\tau_2 - \tau_1}\right)^3, & \text{for } \tau_1 \le t \le \tau_2, \\ p_2\left(\dfrac{t - \tau_2}{\tau_3 - \tau_2}\right)^2, & \text{for } \tau_2 \le t \le \tau_3, \\ 0.0, & \text{for } \tau_3 \le t \le \tau_4, \\ p_3\left(\dfrac{t - \tau_4}{\tau_5 - \tau_4}\right), & \text{for } \tau_4 \le t \le \tau_5, \\ 0.0, & \text{for } t \ge \tau_5. \end{cases}$$

The following specific values are assumed in Eqs. (5.1):

$$p_1 = 0.2\,\mathrm{MPa}, \quad p_2 = 0.3\,\mathrm{MPa}, \quad p_4 = 0.4\,\mathrm{MPa}, \quad \tau_1 = 4\,\mathrm{ms},$$

$$\tau_2 = 6.7\,\mathrm{ms}, \quad \tau_3 = 14.6\,\mathrm{ms}, \quad \tau_4 = 18\,\mathrm{ms}, \quad \tau_5 = 21.3\,\mathrm{ms}.$$

The solution will provide a space-time distribution of deformations and the displacement of the cross-section under direct applied load. The discrete model described in Sec. 3 will be employed. The bar is divided into the segments $\Delta x = 0.1\,\mathrm{m}$. From the condition of the errorless difference approximation it follows that the associated time step is $\Delta t = 0.6667\,\mathrm{ms}$.

The solution is depicted in the phase plane, Fig. 7a. Characteristic regions are designated in the following way: O – a part with no load, I – loading part, II – rigid unloading part. The parts I and II are separated by a line which is here called a rigid unloading wave. With its help the changes of location of the front of rigid region can be situated. The diagram for the travel of the rigid unloading wave is similar to that describing the load variations $p(t)$.

It is not only a single stiffening of a certain part of the bar that takes place in the considered example. Due to a complex load function $p(t)$, a portion of the bar with the length l_{cx} undergoes alternating stiffening and activation. The proposed method copes well with such a situation. The spatial distribution of permanent strains as a result of consecutive passes of the rigid unloading front is also shown in Fig. 7a.

A time-dependent distribution of the stress $\sigma_c(t)$ at the front of rigid unloading is shown diagrammatically in Fig. 7b. Both the stress and the mass velocity of an increasing rigid region are found to decrease. Conversely, as the rigid region shrinks, the stress $\sigma_c(t)$ and the mass velocity increase. The solution presented above is compared with that obtained for a prismatic bar (dashed line). The influence of variable cross-section of the bar on the general behaviour is clearly seen. It can be also noticed that a nonprismatic

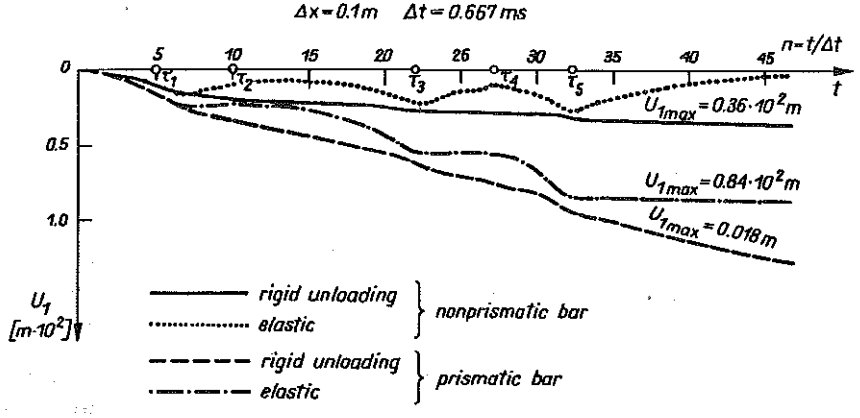

FIG. 8.

bar undergoes a faster stiffening in the unloading process. The reason is a successive enlargement of the current mass of the bar (geometrical damping). To maintain the same dimensions of the unloading region as for a prismatic bar, suitable larger load would be necessary to be applied.

Time-dependence of the displacements u_i of the boundary mass at which the applied load is depicted in Fig. 8. The displacements corresponding to the cases shown in Fig. 7 are compared with solutions suitable for elastic bars. Attention is drawn to the fact that the end displacements depend heavily on the variability of the cross-section and the deformability of the material.

Ten times shorter geometrical step was found to cause no appreciable changes in the solutions visualized in Fig. 7 and 8.

EXAMPLE 2

Consider an undeformable mass M located at the edge section ($x = 0$) of a nonprismatic bar. Geometrical and mechanical parameters are assumed to be the same as in the example 1. The mass M is directly acted upon by an external load $p(t)$ in the form

$$p(t) = p_0 \left(1 - \frac{t}{\tau}\right)^{\beta}, \tag{5.2}$$

where $p_0 = 1.2\,\mathrm{MPa}$, $\tau = 15\,\mathrm{ms}$, $\beta = 3$.

Variations in time $U_M(t)$ of the considered mass will be analysed. Discrete modelling will be used as in the example 1. Addition of the mass M constitutes a global model of the considered problem in accordance with the rules presented in Sec. 3 and in [12]. In this model the value of the first mass will be modified to become

$$\mathcal{M}_1 = \Delta m_1/2 + M. \tag{5.3}$$

To be specific, let us assume $M = 3.75\,\mathrm{t}$. The solution of the problems is shown diagrammatically in Fig. 9. The diagrams *1–6* refer to a nonprismatic bar, the diagrams *7* and *8* correspond to a bar with constant cross-section. The displacement diagram for the assumed specific data is designated by *1*. For the sake of comparison, other displacement diagrams are shown to enable the influence of the value M and the wave velocity a_1 to be evaluated. Effects of the values of mass M are illustrated in the diagrams *2* and *3* ($M = 8\,\mathrm{t}$ and $M = 2\,\mathrm{t}$, respectively). Effects of the wave velocity a_1 are shown in the diagrams *4* and *5* ($a_1 = 300\,\mathrm{m/s}$ and $a_1 = 75\,\mathrm{m/s}$, respectively). A general

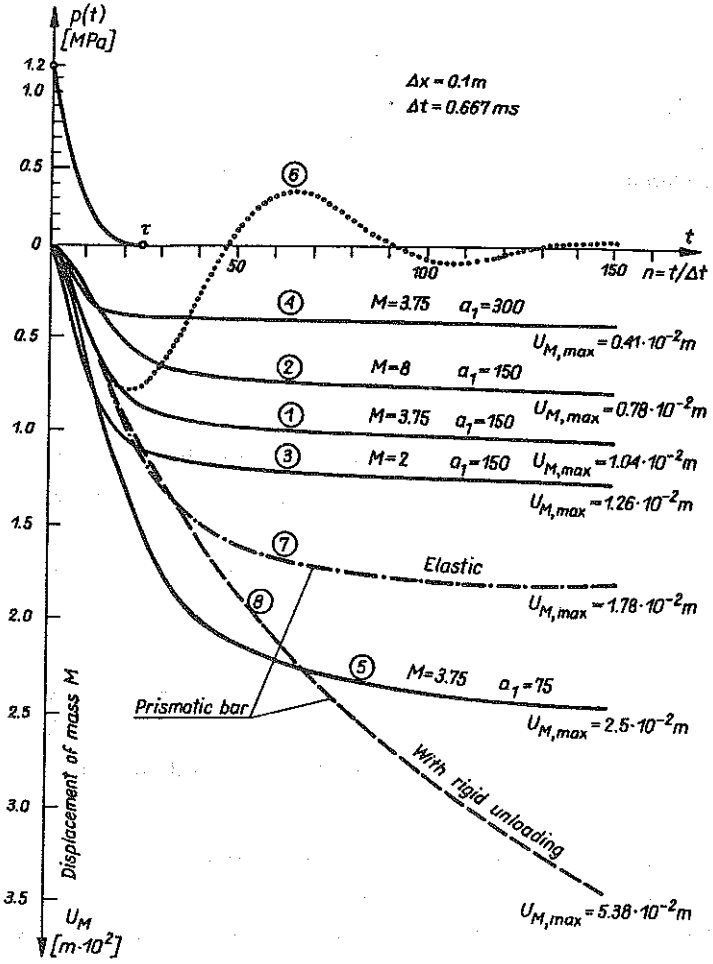

FIG. 9.

conclusion can be drawn that the time-variability of displacements and their maximum values are more sensitive to the changes of the wave velocity a_1 than to the changes of the mass M. This means that the impendance of the material and the geometrical damping are of primary importance in the considered problem.

An influence of elastic properties of the bar material is shown in the diagram *6* (all the specific data are here the same as for the diagram *1*).

The results for a prismatic bar are also presented; the behaviour of an elastic bar is shown in diagram *7* and the rigid unloading is allowed for in the diagram *8*.

The obtained results show a considerable influence of the variable cross--sections and mechanical properties of the bar material. In the considered problem and for the material with a rigid unloading characteristic, the maximum displacements of the mass in a prismatic bar are as many as 5.17 times larger than those in a nonprismatic bar.

6. Conclusions

The principles of discrete modelling of one dimensional wave propagation in a linearly elastic material, i.e. insensitive to whether loading or unloading takes place, were put forward in [12].

Similar model is proposed in this paper for a material exhibiting rigid behaviour upon unloading. Effective solutions can be arrived at as illustrated by an example of Sec. 5.

Both models, described in [12] and here, are capable of solving problems in which the $\sigma - \varepsilon$ relationship is linear, one-segmental and the processes of loading and unloading take place. These elastic and plastic models can be termed the basic ones.

The difficulties typical for such a class of problems tackled analytically, can be overcome automatically so the models can be useful in some more complicated analyses as well. The presented models can be also combined to enable analyses of wave processes in the case of piece-wise linear multi-segmental approximations of the $\sigma - \varepsilon$ relationship, both for loading and unloading. This is particularly convenient for soils subjected to arbitrary dynamic loads without imposing limit on stresses. Propagation of plane, cylindrical and spherical waves may also be dealt with. Discretization of the problem of "plastic gas" published in [20] can also be approached. This model was used in [21] to analyse wave propagation phenomena in soils under very high pressures.

Another field of application of the basic models is the dynamic soil-structure interaction. Cavitation and layered structure of soil can be allowed for.

The results of examples given in Sec. 5 indicate the possibilities of the model to effectively analyse parameters of the motion of structures in the surrounding soil.

REFERENCES

1. A.W.T.DANIEL, R.C.HARWEY and E.BURLEY, *Stress-strain characteristic of sand*, J. Geotechn. Eng. Div., V, 1975.
2. **Г.В.РЫКОВ и А.М.СКОБЕЕВ, Измерение напряжений в грунтах при кратковременных нагрузках, Изд. Наука, Москва 1978.**
3. F.DARVE, *Une description du comportement cyclique des solides non visqueux*, J. de Mec. Theor. et Appl., 1982.
4. W.K.NOWACKI, *Stress waves in nonelastic solids*, Pergamon Press, Oxford 1978.
5. W.K.NOWACKI, *Ondes dans les milieux non-elastiques*, Inst. de Mécanique de Grenoble, 1978.
6. Z.DŻYGADŁO, S.KALISKI, L.SOLARZ and E.WŁODARCZYK, *Vibrations and waves in solids* [in Polish], PWN, Warszawa 1966.
7. S.KALISKI, J.OSIECKI, *Unloading wave for a body with rigid unloading characteristic*, Proc. Vibr. Probl., 1, 1959.
8. E.WŁODARCZYK, *Propagation and reflection of one- and two-dimensional stress waves in plastic bodies* [in Polish], Biul. WAT, 198, 2, Warszawa 1969.
9. **М.Д.БОДАНСКИЙ, Л.М.ГОРШКОВ, В.И.МОРОЗОВ и В.С.РАСТОРГУЕВ, Расчет конструкций убежищ, Строиздат, Москва 1974.**
10. Z.ŁĘGOWSKI, K.PODOLAK and E.WŁODARCZYK, *Effects of explosion on a structure immersed in soil* [in Polish], Biul. WAT, 7, 1975.
11. A.PAPLIŃSKI and E.WŁODARCZYK, *Interaction of elastic-plastic stress waves with an incompressible plane layer resting on an elastic half-space* [in Polish]; Rozpr. Inż., **20**, 2, 1972.
12. G.BĄK and Z.SZCZEŚNIAK, *Discrete modelling of one-dimensional wave processes in elastic layered nonprismatic bars* [in Polish], Rozpr. Inż., **35**, 2, 1987.
13. G.BĄK and Z.SZCZEŚNIAK, *Modelling of splinters and multiple impacts in elastic-brittle bars under tension* [in Polish], Rozpr. Inż., **37**, 1, 1989.
14. P.GUELIN and W.K.NOWACKI, *Stress waves in elastic-plastic solids with discrete memory*, J. Techn. Phys., **33**, 2, 1992.
15. E.WŁODARCZYK, *Models of rocks and soils in wave problems. Part I. Elastic and elastic-plastic models. Part II. Viscous and plastic-viscous models* [in Polish], Arch. Inż. Ląd., 3/4, 1991.
16. **Г.М.ЛЯХОВ, Основы динамики взрыва в грунтах и жидких средах, Изд. Недра, Москва 1964.**
17. **Б.В.ЗАМЫШЛЯЕВ и Л.С.ЕВТЕРЕВ, Модели динамического деформирования и разрушения грунтовых сред, Наука, Москва 1990.**
18. S.KALISKI, W.K.NOWACKI and E.WŁODARCZYK, *On a certain closed solution for shock-wave rigid unloading*, Bull. Acad. Polon. Sci., Série Sci. Techn., **15**, 5, 1967.

19. R.C.SHIEH, G.A.HEGEMIER and W.PRAGER, *Closed-form solutions to problems of wave propagation in a rigid, workhardening, locking rod*, Int. J. Solids Struct., 5, 1969.

20. **Х.А.РАХМАТУЛИН, О распространении волн в многокомпонентных средах, П.М.М., 33**, 4, 1969.

21. W.K.NOWACKI and B.RANIECKI, *Theoretical analysis of dynamic compacting of soil around a spherical source of explosion*, Arch. Mech., **39**, 4, 1987.

22. I.KISIEL, *Dynamics of machinery foundation* [in Polish], PWN, Warszawa 1957.

MILITARY TECHNICAL ACADEMY, WARSZAWA.

Received November 6, 1991.